Polymer Degradation and Stability 190 (2021) 109629

Contents lists available at ScienceDirect

Polymer Degradation and Stability

journal homepage: www.elsevier.com/locate/polymdegradstab

A bi-DOPO type of flame retardancy epoxy prepolymer: Synthesis, properties and flame-retardant mechanism

Dongyue Liu, Pengfei Ji, Tianlong Zhang, Jipeng Lv, Yihua Cui*

College of Materials Science and Technology, Nanjing University of Aeronautics and Astronautics, Nanjing 210016, China

ARTICLE INFO

Article history:
Received 28 December 2020
Revised 10 May 2021
Accepted 16 May 2021
Available online 19 May 2021

Keywords:
Epoxy prepolymer
DOPO
Bisphenol A
Flame-retardant mechanism
Mechanical property

ABSTRACT

A bi-DOPO type of prepolymer for flame retardancy epoxy resins with intrinsically flame-retardant was successfully synthesized by reacting of 6,6′-((6,6′-dihydroxy-[1,1′-biphenyl]-3,3′-diyl) bis (propane-3,1-diyl)) bis(dibenzo[c,e][1,2] oxaphosphinine 6-oxide) (DOBP) with bisphenol A. The characterization of the cured epoxy resins, such as cone calorimeter, TGA/infrared, Raman and SEM indicated that DOBP with double 9,10-dihydro-9-oxa-10-phosphaphenanthrene-10-oxide (DOPO) structure endowed the epoxy resins with excellent flame retardancy, including limiting oxygen index of 40.0%, V-0 rating in UL-94, remarkable smoke suppression and flame inhibition. The quenching effect of gaseous phase and charring effect of condensed phase of phosphaphenanthrene groups in prepolymer together contributed to the improvement on the flame retardant performance of the epoxy resins. In addition, due to the rigid structure of DOBP molecules, the cured *d*-FREP possessed high glass transition temperature of up to 192.9°C, and the tensile modulus of which was increased about 55% compared with the neat epoxy resins.

1. Introduction

It was well known that epoxy resins exhibited excellent adhesion, chemical resistance, electrical insulation, and high strength because of the reasonable ratio of rigid and flexible groups in its molecular structure [1–5]. Epoxy resins have achieved great success in practical applications such as adhesives, coatings, encapsulating materials, building materials. However, like most organic polymer materials, epoxy resins were flammable. For the applications where needed high fire requirement, epoxy resins were greatly confined [6]. Therefore, improving the flame retardancy of the epoxy resins was of great significance to widen its practical applications. Introducing flame retardants was considered to be an effective way to improve the flame-retardant properties of the epoxy resins, such as phosphorus- or nitrogen-containing flame retardants and intumescent flame retardants, etc [7–11].

Among these, 9,10-dihydro-9-oxa-10-phosphaphenanthrene 10-oxide (DOPO) and its derivatives were widely applied in the epoxy resins due to their remarkable flame-retardant effect [12,13]. Schartel et al introduced DOPO-containing flame retardant DOP-Et into the molecular structure of epoxy resins. The results showed that when the content of DOP-Et was 15.7 wt%, the limiting oxygen index of the cured epoxy resins was increased from 21% to 42%, and there was no deterioration in the tensile properties. The interaction between the DOPO-Et and the epoxy resins changed the decomposition mechanism of the epoxy resins and increased the formation of residual carbon. The release of phosphorus-containing product played a role of flame inhibition [14]. The DOPO exhibited remarkable flame-retardant performance because the active free radicals of the flame zone were quenched, and the release of flammable volatiles was inhibited by a char layer containing phosphorous [15–23]. Although the flame-retardant effect of DOPO was remarkable, its compatibility with the epoxy resins was poor.

To solve this problem, it was a great strategy to embed DOPO into epoxy resins skeleton through a chemical reaction [24–28]. Chi et al synthesized a kind of DOPO-contained epoxy prepolymer (TEBA), it was proved that TEBA possessed excellent flame-retardant properties after cured by DDM. Compared with the neat epoxy resins, the LOI of the cured epoxy resins containing TEBA increased from 25.8% to 42.3%, the tensile strength and glass transition temperature of the cured epoxy resins containing TEBA decreased by 16% and 18%, respectively [29]. Although the problem of poor compatibility of flame-retardant with epoxy resins was solved, due to the asymmetry of the DOPO molecular structure, the glass transition temperature (T_g) and mechanical properties of the epoxy resins were often deteriorated, which greatly hindered the practical applications of the epoxy resins. It was challenging to design new type of epoxy resins with both high-efficiency flame-retardant and excellent mechanical properties [30–34].

* Corresponding author.
E-mail address: cuiyh@nuaa.edu.cn (Y. Cui).

https://doi.org/10.1016/j.polymdegradstab.2021.109629
0141-3910/

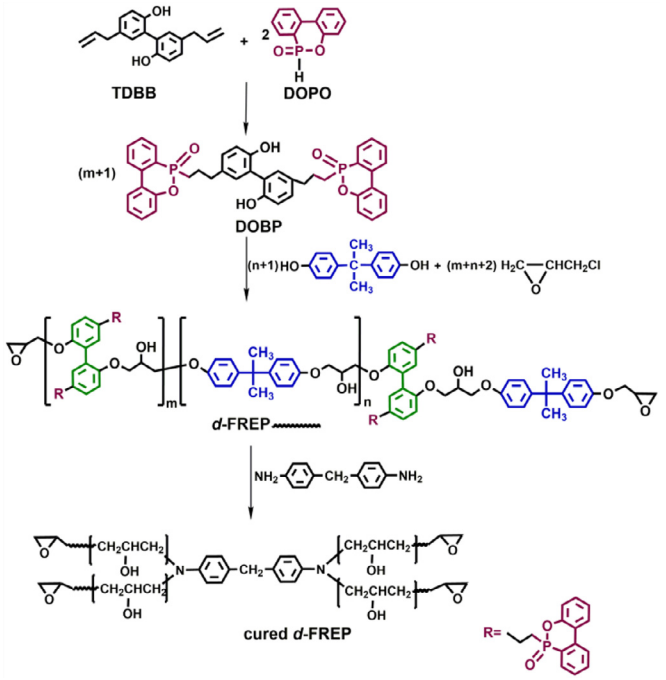

Fig. 1. The preparation processes of DOBP, *d*-FREP, the cured *d*-FREP.

In this study, epoxy prepolymer with DOPO group (*d*-FREP) was synthesized by reacting of DOBP with bisphenol A and epichlorohydrin. Moreover, the flame-retardant properties, mechanical properties and glass transition temperature of the cured *d*-FREP were studied. The flame-retardant mechanism of the cured *d*-FREP was analyzed.

2. Experimental

2.1. Materials

Epichlorohydrin (ECH), tetrabutylammonium bromide, dichloromethane, sodium hydroxide and bisphenol A were provided by Sinopharm Chemical Reagent Co, Ltd. 9, 10-Dihydro-9-oxa-10-phosphaphenanthrene-10-oxide (DOPO) was obtained from Zhengzhou Chengtong Chemical. Magnolol (5′,5-diallyl-2,2′-hydroquinone) was purchased from Nanjing Jingzhu Biotechnology Co, Ltd. The bisphenol A type epoxy resins (commercial name: E-51) was provided by Bluestar New Material Wuxi Resin Factory. 4,4-diaminodiphenylmethane (DDM) was purchased from Disney's Aladdin. All chemicals and solvents were used directly without further purification.

2.2. Synthesis of DOBP

Firstly, DOPO (47.56 g, 0.22 mol) was melted under 120°C, and then magnolol (30.84 g, 0.10 mol) was added into the flask containing DOPO. The air in the flask was replaced by nitrogen (N_2). Then, the addition reaction of DOPO and magnolol was occurring at 160°C for 24 h. The crude product was absolutely dissolved in ethanol (100 mL) and was washed with hot deionized water (90°C). This washing procedure was repeated for four times. The 6,6′-((6,6′-dihydroxy-[1,1′-biphenyl]-3,3′-diyl) bis (propane-3,1-diyl)) bis(dibenzo[c,e] [1,2] oxaphosphinine 6-oxide) (DOBP) was obtained after dried at 80°C for 24h in vacuum oven and used for the synthesis of *d*-FREP. The synthesis route of DOBP was illustrated in Fig. 1. For the characterization of NMR, the column chromatography (silica gel, ethyl acetate/methanol = 15/1) was carried out to get the purified DOBP.

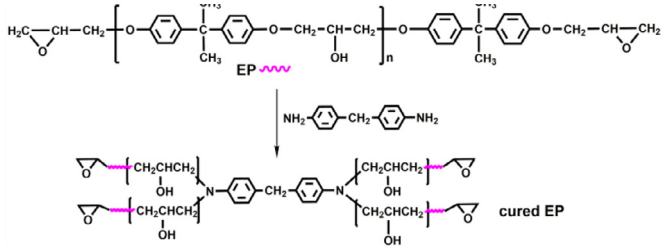

Fig. 2. The preparation processes of the neat epoxy resins.

2.3. Synthesis of d-FREP

14.20 g DOBP, 4.57 g bisphenol A, and 185.04 g ECH were added into a three-port flask, and then kept stirring until DOBP was completely dissolved. After that, tetrabutylammonium bromide (0.77 g) was added. The reaction was occurring at 60°C for 2 h. Subsequently, 25% sodium hydroxide solution was added and reacted at 75°C for 2 h. To remove the sodium chloride, the crude product was dissolved in dichloromethane and washed with hot water (65°C) for four times. The purified epoxy prepolymer (*d*-FREP) was obtained after removing dichloromethane and epichlorohydrin by rotary evaporation. The epoxy equivalent of the *d*-FREP was 312 g/mol. The synthesis route of *d*-FREP was illustrated in Fig. 1.

2.4. Curing of the d-FREP and the neat epoxy resins

DDM was used as the curing agent of the *d*-FREP. The *d*-FREP was mixed with DDM in a 4:1 equivalent ratio. The mixture was degassed by vacuum process for 3 min, then the mixture was poured into the Teflon molds and cured at 115°C for 2 h, 160°C for 2 h and 210°C for 2 h. The phosphor content in the cured *d*-FREP was determined by ICP-OES (0.22%). The cured route of *d*-FREP was illustrated in Fig. 1. The curing temperature of the *d*-FREP was predetermined by DSC nonisothermal thermograms (Table S1).

The epoxy resins (diglycidyl ether of bisphenol-A, epoxy value 0.51) was heated to 120°C. Then, DDM was added into the epoxy resins at 110°C and stirring for 3min. The mixture of the epoxy resins and DDM was transferred to a vacuum oven at 110°C for degassing. Finally, the gas-free mixture was poured into a Teflon mold. It was then cured in a vacuum oven at 115°C for 2 h, 160°C for 2 h and 210°C for 2 h. The cured route of the neat epoxy resins was illustrated in Fig. 2.

2.5. Characterization

2.5.1. Structural characterization

Fourier transform infrared (FTIR) of the DOBP and the *d*-FREP were obtained by a FTIR-8400S (Shimadzu) spectrometer using KBr pellets method. The range of wave numbers were 4000-500 cm^{-1}, and the resolution was 1 cm^{-1}.

Nuclear magnetic resonance (NMR) spectra of DOBP and *d*-FREP were detected at room temperature using a Bruker DRX 500 spectrometer operated under 500 MHz. The NMR specimen was prepared by dissolving 30 mg sample in deuterated dimethyl sulfoxide (DMSO-d_6) (500 μL).

Elemental analysis of DOBP was obtained by a Vario EL elemental analyzer (Elementar Analysensysteme GmbH, Germany) with a combustion temperature at 900°C. The results were the average of the 2 times repeated tests.

Mass spectroscopy (MS) was performed via an Agilent LC-MS 1290uplc spectrometer, with the high-resolution MS data was obtained by an Agilent qtof6550 apparatus.

The melting points of DOBP were obtained on a Yanagimoto micro melting point apparatus without correction.

2.5.2. Epoxide equivalent weights (EEW)

The epoxide equivalent weights (EEW) of the *d*-FREP were obtained from HCl/acetone titration method according to HGZ-741-72. 0.5 g *d*-FREP was dissolved in 20 mL solution containing HCl and acetone and stored for 30 minutes before titration. Then, 6-8 drops phenolphthalein used as indicator. 0.1 mol/L ethanol solution containing sodium hydroxide was used to titrate.

2.5.3. Phosphorus content

Phosphorus content of the cured *d*-FREP was measured by inductively coupled plasma optical emission spectrometer (ICP-OES) according to Agilent 720ES. 150 mg powder of the cured *d*-FREP was completely combusted into gas under oxygen atmosphere, and then the volatile was absorbed by 25 ml 0.001 mol/L $KMnO_4$ aqueous solution, and then was diluted to 100 ml with deionized water.

2.5.4. Flame retardancy and fire behavior

The LOI value of the cured *d*-FREP and the neat epoxy resins were measured using a K-R2406S according to ASTM D2863-00. The sheet dimension of each sample was 130.0 × 6.5 × 3.2 mm^3.

The UL-94 of the cured *d*-FREP and the neat epoxy resins were carried out in an XWW-20A instrument according to ASTM D3801/UL-94 and the sheet dimension of each sample was 130.0 × 13.0 × 3.2 mm^3.

The fire behavior of the cured *d*-FREP and the neat epoxy resins were studied using a FTT cone calorimeter according to ISO 5660-1. The samples with a size of 100.0 × 100.0 × 3.0 mm^3 were exposed to a radiant cone (35 kW/m^2).

2.5.5. Differential scanning calorimetry (DSC)

The glass transition temperature of the cured *d*-FREP and the neat epoxy resins were determined under N_2 atmosphere via the differential scanning calorimetry (DSC) of the 214 Polyma. The heating temperature range was 40-250°C, and the heating rate was 10°C/min. 8 ± 0.5 mg powder sample was used in the test of DSC.

The mixed liquids (around 5-8 mg) of the *d*-FREP and DDM were used in the research of nonisothermal curing kinetics. The heat scan ranging from 50°C to 250°C was performed at varying heating rates of 5°C/min, 10°C/min, 15°C/min, and 20°C/min, respectively.

2.5.6. Thermogravimetric analyzer (TGA)

The thermogravimetric analysis (TGA) of the cured *d*-FREP and the neat epoxy resins were carried using a Netzsch thermogravimetric analyzer. 5 ± 0.5 mg powder samples were heated from 40°C to 700°C with a heating rate of 10°C/min under a nitrogen flow.

2.5.7. Char residue analysis

The morphologies of the char residues (inner surface and outer surface) of the cured *d*-FREP were observed by S-3400NII scanning electron microscope (SEM) at an acceleration voltage of 10 kV. The char residues were coated a conductive Au layer.

Raman spectrum of char residues powder was performed on a LabRam HR Evolution Raman spectrometer with excitation wavelength at 532 nm.

2.5.8. Gaseous analysis

Thermogravimetric analysis/infrared spectrometry (TGA-IR) of the neat epoxy resins and the cured *d*-FREP were performed using the TG209F3/TENSOR 27. About 9.0 mg of each sample powder was put in an alumina crucible and heated from room temperature to 700°C at a heating rate of 20°C/min (nitrogen atmosphere, the flow rate of 50 mL/min).

2.5.9. Mechanical property test

According to ASTMD-638, the tensile strength and elastic modulus of the cured *d*-FREP and the neat epoxy resins were evaluated on an XWW-20A universal testing machine. The selected load was 5000 N and the stretching rate was 3 mm/min. The dimensions of the specimen were 75 mm × 5 mm × 2 mm. The tensile properties of the samples were the average of five measured values.

Notched Izod impact strength of the samples was measured with a XJ-300Aimpact tester according to the ISO 179-1. The thickness of the notched impact bars was 4 mm, and the impact energy was 1 J.

3. Results and discussion

3.1. Characterization of DOBP and d*-FREP*

The chemical structure of DOBP was characterized by FTIR. After the reaction of DOPO with magnolol, new peaks, such as 1438 cm^{-1} P-C bond, 1030 cm^{-1} P-O bond, P-Ph bond (1595 cm^{-1} and 1476 cm^{-1}), P-O-C bond (907 cm^{-1}), and -CH_2 bond at 2932 cm^{-1}, phenolic hydroxyl group (3403 cm^{-1}) were appeared, as shown in Fig. S2. At the same time, C=C (1641 cm^{-1}) in magnolol and P-H (2432 cm^{-1}) in DOPO were disappeared, indicating that the DOBP was obtained by an addition reaction between P-H bond of DOPO and C=C bond of magnolol.

The *d*-FREP was prepared by the reaction of DOBP, bisphenol-A, and epichlorohydrin. The phenolic hydroxyl (3411 cm^{-1}) in DOBP were disappeared as shown in Fig. S2. Meantime, the new characteristic absorption peaks of phosphaphenanthrene were appeared in 1271 (P=O), 1035 (P-O), and 1437 cm^{-1} (P-C). The absorption bands at 1508, 1243, 913 and 858 cm^{-1} belonged to the epoxy group. These results indicated that *d*-FREP was successfully prepared.

The chemical structure of the DOBP was further verified by ^{1}H-NMR, ^{13}C-NMR and ^{31}P-NMR spectra. In Fig. 3A, the ^{13}C-NMR (DMSO-d_6, δ): the chemical shifts at 24.1 ppm were assigned to the methylene; the chemical shifts at 26.51-27.55 ppm were ascribed to the methylene near benzene; the chemical shifts at 149.6 ppm, 120.45 ppm -120.60 ppm, 131.23 ppm, 124.9 ppm, 125.88 ppm, 135.00 ppm, 120.46 ppm -120.62 ppm, 131.8 ppm, 128.3 ppm, 133.75 ppm, 125.15 ppm, 124.65-124.88 ppm came from the signal of -CH_2 in phosphaphenanthrene; the chemical shifts at 126.18 ppm, 134.90 ppm -135.05 ppm, 122.2 ppm -122.44 ppm, 153.00 ppm, 116.2 ppm were corresponded to the trisubstituted benzenes; the chemical shifts at 153.00 ppm were attributed to the -CH_2 group close to the phenolic -OH.

From the ^{1}H-NMR (DMSO-d_6, δ), the chemical shifts at 9.03 ppm were ascribed to the phenolic -OH, as shown in Fig. 3B. The chemical shifts at 7.25-8.25 ppm were corresponded to the aromatic-H in phosphaphenanthrene. The chemical shifts at 6.70-6.95 ppm were assigned to -CH_2 in the trisubstituted benzene. The chemical shifts at 2.52-2.5 ppm were ascribed to the methylene close to the phenanthroline. The chemical shifts at 2.12-2.21 and 1.65-1.79 ppm were caused by methylene near benzene.

As shown in Fig. 3C, the ^{31}P-NMR (DMSO-d_6, δ) spectrum exhibited signals at 37.51 ppm, which were assigned to phosphaphenanthrene. The chemical shift and integrated area of each peak were consistent with the number of protons in the DOBP chemical structure.

The element content of DOBP (calculated/experimental, %), C: 72.20/72.14 ± 0.05; H: 5.17/5.21± 0.03. The melting point of the DOBP: 113-116°C. The positive mode of ESI-MS spectrum of DOBP (Fig. S3) gave the quasi-molecular ion peak $[M+H]^+$ at m/z 699.2037 (calcd. for $C_{42}H_{36}O_6P_2H$ 699.2000). The results showed that the target product DOBP was successfully synthesized.

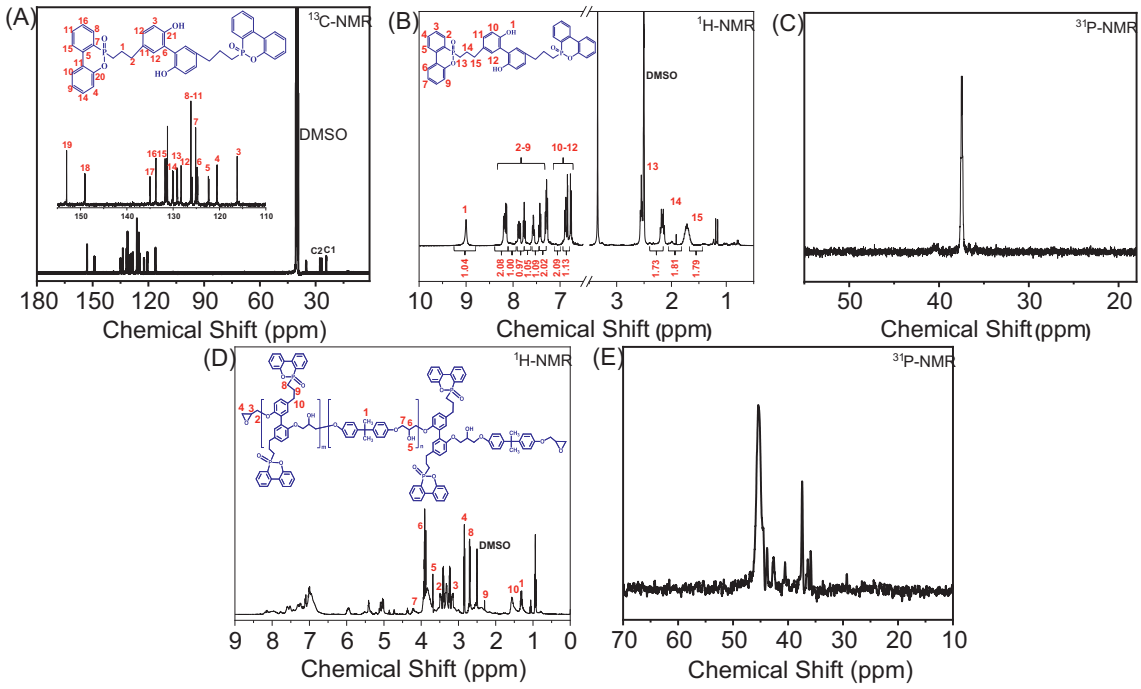

Fig. 3. The ^{13}C-NMR spectra of DOBP (A), the ^{1}H-NMR spectra of DOBP (B) and *d*-FREP (D), ^{31}P-NMR spectra of DOBP (C) and *d*-FREP (E).

The chemical structure of the *d*-FREP was further verified by ^{1}H-NMR and ^{31}P-NMR spectra. From the ^{1}H-NMR (DMSO-d_6, δ) spectra (Fig. 3D), the chemical shifts at 7.1 ppm-8.3 ppm were ascribed to the aromatic-H of phosphaphenanthrene group; the chemical shifts at 2.52 ppm-2.57 ppm were corresponded to the -CH_2 near the phosphaphenanthrene group; the chemical shifts at 2.29~2.30 ppm were caused by the H vibration of -CH_2 far away from phosphorus; the chemical shifts at 6.7-7.1 ppm were ascribed to the aromatic-H of the benzene ring. Three sets of resonance signals at 3.50, 3.25 and 2.82 ppm can be distinguished from the ^{1}H-NMR spectrum, which were assigned to the protons of -CH (2) and -CH_2- (3,4) of the epoxy group. A signal at 1.55 ppm can be observed and assigned to the protons (1) of methyl on bisphenol-A. The signal at 3.58 ppm (5) was attributed to the appearance of hydroxyl, and the signals at 3.95 and 4.25 ppm (6, 7) were assigned to -CH and -CH_2- on -O-CH_2-CH (OH)-, respectively.

Fig. 2E shown the ^{31}P-NMR (DMSO-d_6, δ) spectrum of *d*-FREP. The peaks at 45.51 ppm and 37.51 ppm were derived from the DOPO group of the *d*-FREP, corresponding to the phosphorus atom near the epoxy group and the phosphorus atom near the ether bond, respectively. The ^{31}P-NMR of *d*-FREP got multiple peaks close to each other. This was due to the steric hindrance effect of bulky DOPO pendant and the existence of chiral carbon atom, which might result in the formation of diastereomers with unequal phosphorus peaks [35–37]. Based on the results and analysis above the *d*-FREP was synthesized successfully.

3.2. Thermal decomposition and fire behavior

The TGA and DTG curves of the cured *d*-FREP and the neat epoxy resins under the nitrogen atmosphere were illustrated in Fig. 4. The temperature at the mass loss of 5% ($T_{5\%}$), the decomposition temperature at the first stage (T_1), the decomposition temperature at the second stage (T_2), the maximum mass loss rate (R_{max}) and the residual mass at 700°C (Residual) were listed in Table 1.

The cured *d*-FREP exhibited a lower $T_{5\%}$ and T_1 than that of the neat epoxy resins as shown in Table 1, which was probably because the O=P-O bond of the cured *d*-FREP was less stable than that of the C-C bond [29,34,38,39]. In Fig. 3(b), the neat epoxy resins presented a typical one-stage decomposition of around 395.7°C. However, a two-stage decomposition of the cured *d*-FREP can be observed from the DTG curve at 384.1°C (T_1) and 507.4°C (T_2), respectively. According to the pyrolysis characteristics of the cured *d*-FREP, the first stage of the weight loss might be characteristic decomposition of the joint epoxy resins structure. In the second stage, some of the phosphoryl-substituted aromatics were evaporated [28]. Compared with the neat epoxy resins, the R_{max} of the cured *d*-FREP was decreased from 2.3 wt%/°C to 0.4 wt%/°C. In addition, the char residue of the cured *d*-FREP (28.5%) was significantly higher than that of the neat epoxy resins (14.3%) and also the existing the epoxy resins of flame retardant [12,40,41], which showed that the cured *d*-FREP possessed efficient carbonization capacity.

Table 1 and Table 2 shown the LOI values and UL-94 ratings of the cured epoxy resins. The neat epoxy resins were failed to self-extinguish, accompanied by dripping during the combustion process. Thus, the neat epoxy resins did not achieve any classification in the UL-94 test. However, the cured *d*-FREP can automatically extinguish within 3s for the first ignition, and cannot be ignited for the second ignition. Consequently, the cured *d*-FREP can passe the V-0 rating in UL-94 test. The LOI value of the cured *d*-FREP (40.0%) was higher than that of the neat epoxy resins (21.0%) and also the existing epoxy resins of flame retardancy [12,40,41]. These results indicated that the cured *d*-FREP possessed excellent flame retardancy.

In order to gain a deeper understanding of fire behavior of the cured *d*-FREP, the burning characteristic parameters of the cured *d*-FREP and the neat epoxy resins were recorded by the CONE, including heat release rate (HRR), peak of the HRR (PHRR), total heat release (THR) and the time to ignition (TTI). Simultaneously, the total production of smoke (TSP), smoke release rate (SPR), mass loss rate (MLR), and average effective heat of combustion (av-EHC) can also be obtained by CONE test.

The TTI value of the cured *d*-FREP was decreased compared with the neat epoxy resins as shown in Table 3. This result implied

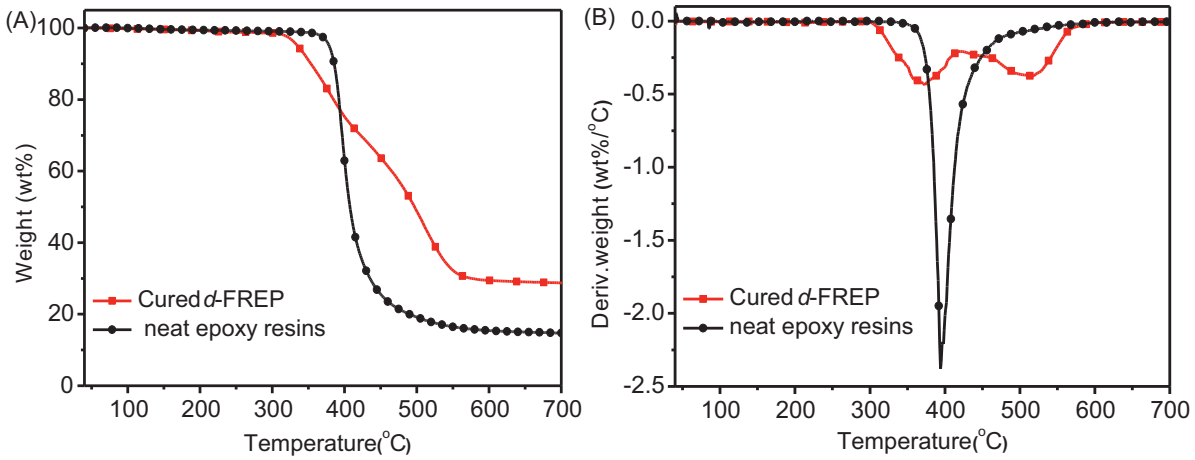

Fig. 4. TGA (A) and DTG (B) curves of the neat epoxy resins and the cured *d*-FREP under nitrogen atmosphere.

Table 1
Thermal decomposition parameters, T_g and LOI data of the neat epoxy resins, the cured *d*-FREP, and other cured epoxy prepolymers of flame retardant.

Sample	Phosphorus content (%)	$T_{5\%}$ (°C)	T_1 (°C)	T_2 (°C)	R_{max} (wt%/°C)	Residual (%)	T_g (°C)	LOI (vol %)
Neat epoxy resins	0	378.4	395.7	-	-2.3	14.3	151.9	21.0±0.2
Cured *d*-FREP	0.22	346.3	384.1	507.4	-0.4	28.5	192.9	40.0±0.2
DOPO-EP1 [40]	8	330.0	-	-	-	24.2	145.0	46.0
DOPO-EP2 [40]	4.4	338.0	-	-	-	18.0	131.0	38.5
EADI-P4.4 [12]	4.4	288.5	-	-	-	6.5	101.9	22.8
PPR-EP [41]	4.1	360.0	-	-	-	16.7	109.0	30.1

Table 2
The UL-94 level of the neat epoxy resins and the cured *d*-FREP.

Samples	UL-94 (3.2 mm)		
	t_1+t_2(s)[a]	Dripping	Rating
Neat epoxy resins	Lasting burning	Yes	NR
Cured *d*-FREP	3+0	No	V-0

[a] Combustion duration after the first (t_1) and the second ignition (t_2).

Table 3
Cone calorimeter results of the neat epoxy resins and the cured *d*-FREP.

Sample	Neat epoxy resins	Cured *d*-FREP
TTI(s)	85±3	38±2
PHRR (kW/m^2)	957±49	272±31
THR (MJ/m^2)	96.7±1.5	34.8±0.8
FIGRA (kW/(m^2•s))	5.35	4.88
TSP (m^2)	34.70±1.61	25.50±1.59
av-EHC (MJ/kg)	22.0±0.9	12.9±1.5
MLR (g/s)	0.11±0.01	0.06±0.01
Residue (wt%)	11.6±0.8	28.6±1.3
CO (kg/kg)	0.04±0.01	0.15±0.01
CO_2 (kg/kg)	1.5±0.1	0.8±0.1

that the phosphaphenanthrene group can catalyze the pyrolysis of the cured *d*-FREP at the early stage, which was consistent with the TGA results. Fig. 5A and B showed the HRR and THR curves of the neat epoxy resins and the cured *d*-FREP. The HRR was an important parameter to evaluate the intensity of combustion. It was notable that the cured *d*-FREP showed the lower PHRR than that of the neat epoxy resins. Moreover, two peaks appeared in the HRR curve of the cured *d*-FREP, similar to what was previously reported for the other type of the flame retardant epoxy resins [29,42–44]. The first peak and the second peak respectively appeared at 49 s and 78 s, and the corresponding PHRRs were 241 kW/m^2 and 272 kW/m^2, respectively. However, the neat epoxy resins showed a single PHRR of 957 kW/m^2 in 179 s.

Furthermore, the fire hazard of the epoxy resins was estimated by FIGRA, which was equal to the maximum value of HRR(t)/t. Compared with the neat epoxy resins, the FIGRA of the cured *d*-FREP was reduced from 5.35 kW/(m^2•s) to 4.88 kW/(m^2•s). The cured *d*-FREP showed the low THR value of 34.8 MJ/m^2 and high char residue (28.6%) compared with the neat epoxy resins (THR: 96.7 MJ/m^2 and char residue: 11.6%). It was mainly because the decomposition of the cured *d*-FREP generated the phosphorus-containing acid, which catalyzed the carbonization reaction and endothermic dehydration of the epoxy resins. Besides, compared with the neat epoxy resins, the MLR of the cured *d*-FREP was reduced by 45% (from 0.11 g/s to 0.06 g/s). This result suggested that the carbonaceous layer can effectively inhibited the transfer of mass, heat and oxygen. More final residue implied that the char layer not only enhanced the protective effect but also the fuels release to gaseous phase was reduced. Therefore, compared with the neat epoxy resins, the combustion intensity of the cured *d*-FREP was effectively suppressed during the test, a small amount of heat was released. The results above proved that the cured *d*-FREP presented better fire safety and lower fire propagation rate than that of the neat epoxy resins.

Compared with the neat epoxy resins, the av-EHC of the cured *d*-FREP (12.9 MJ/kg) was decreased by nearly 41%, which indicated that more significant flame retardant effect of gaseous phase was existed in the cured *d*-FREP. It was believed that the PO• radicals released during the pyrolysis process of the cured *d*-FREP captured the H• and HO• radicals, insufficient combustion was happened, and thereby the chain reaction of free radicals during combustion of the cured *d*-FREP was inhibited. Moreover, the carbon monoxide yield of the cured *d*-FREP was significantly increased, while the carbon dioxide yield was reduced compared with the neat epoxy resins. This verified the flame inhibition effect of the phosphaphenanthrene group was produced in the gaseous phase.

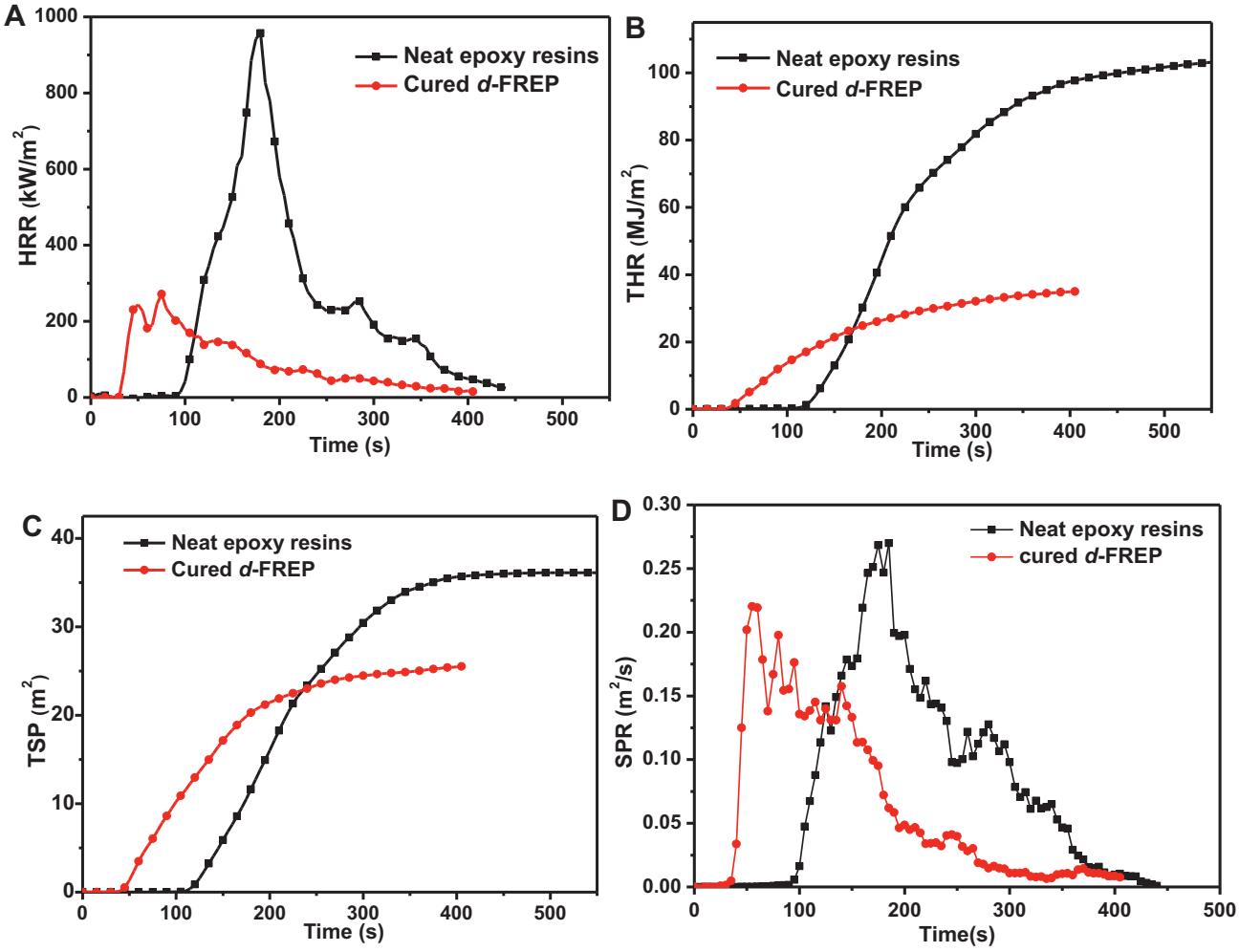

Fig. 5. HRR (A), THR (B), TSP (C) and SPR (D) of the neat epoxy resins and the cured *d*-FREP.

The TSP and SPR of the cured *d*-FREP were lower than that of the neat epoxy resins as shown in Fig. 5C and D, revealing that the introduction of phosphaphenanthrene group enhanced the smoke inhibition of the cured *d*-FREP, which was mainly originated from the charring and flame inhibition effect of phosphaphenanthrene group. Based on the above analysis, the charring (reduction in fuel released) was the minor mechanism (17% reduction) of flame retardancy, the flame inhibition was here the main mechanism (41% reduction).

3.3. Analysis of flame-retardant mechanism in gaseous phase

TGA-FTIR was used to analyze the pyrolysis products of the epoxy resins during thermal decomposition. The FTIR spectra of the pyrolysis products for the neat epoxy resins and the cured *d*-FREP at different temperatures were shown in Fig. 6A and Fig. 6B, respectively, and the related data were shown in Table 4.

It can be proved that the neat epoxy resins began to produce the pyrolysis products at 400°C, as shown in Fig. 6A. The main gaseous pyrolysis products were H_2O (3749 cm^{-1}), methane (3013 cm^{-1}), hydrocarbon compound (2970 cm^{-1}), CO_2 (2360 cm^{-1}), CO (2182 cm^{-1}), aromatic compounds (1507 cm^{-1}, 1600 cm^{-1}) and ethers compounds (1749 cm^{-1}, 1258 cm^{-1} and 1182 cm^{-1}). However, the decomposition of the cured *d*-FREP was occurred at 350°C as shown in Fig. 6B, where the additional absorption bands may be observed, such as 1260 cm^{-1} (P=O) and 1118 cm^{-1} (P-O-P-O). This result together with the TGA results indicated that earlier decomposition of the cured *d*-FREP was caused by the pyrolysis of O=P-O bond.

Table 4
TGA-FTIR spectra of pyrolysis products for the neat EP and the cured *d*-FREP.

Sample	Wavenumber (cm^{-1})	Assignment
Neat EP	3648	O-H
	3013	C-H vibration absorption for CH_4
	2970	C-H of hydrocarbons
	2360	CO_2
	2182	CO
	1749	C=O
	1507, 1600	compounds containing aromatic ring
	1258	aromatic ethers
	1182	compounds containing ethers
	819	C-H for aromatic compounds
Cured d-FREP	3749	H_2O
	1260	P=O
	917	P-O-Ph
	1118	P-O-P-O

After 430°C, there was no significant variation of the type of pyrolysis product of the neat epoxy resins. However, for the cured *d*-FREP, the peak intensity of P=O bond (1260 cm^{-1}) gradually was decreased and the characteristic peak of P-O-Ph (917 cm^{-1}) was appeared in 430°C. This indicated that the polyphosphate structures containing P=O bond can react with phenol of pyrolysis products of gaseous to form the P-O-Ph bond.

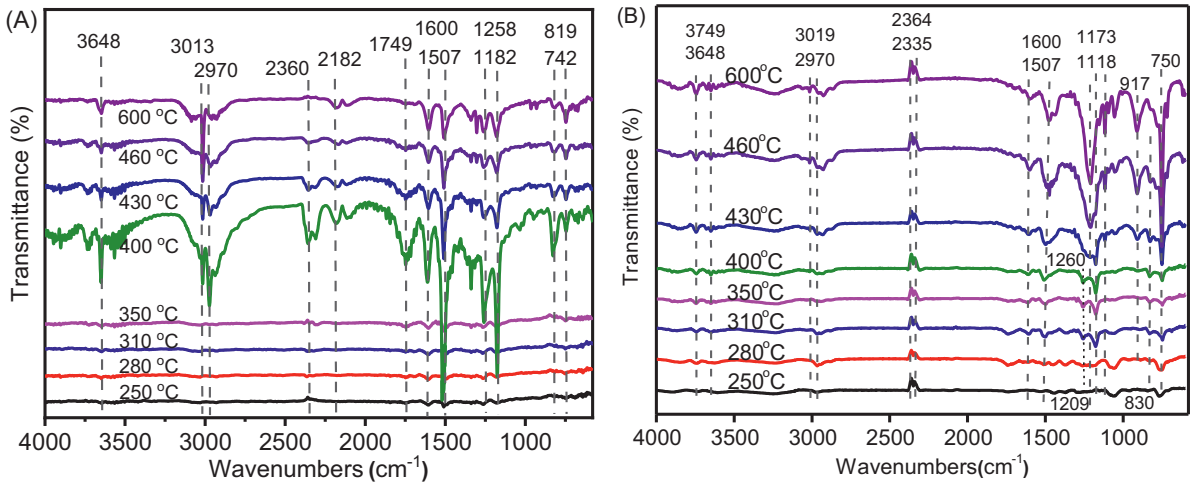

Fig. 6. TGA-FTIR spectra of pyrolysis products for the neat epoxy resins (A) and the cured *d*-FREP (B) at the different temperatures.

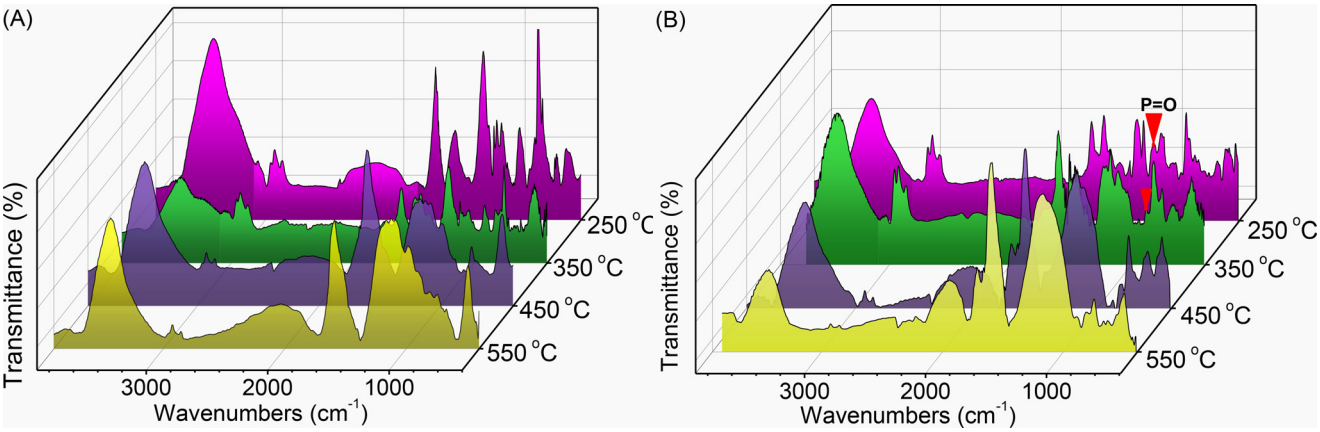

Fig. 7. FTIR spectra of the neat epoxy resins (A) and the cured *d*-FREP (B) under heating at a different temperature in air for 30 min.

Table 5
Assignment of FTIR spectra of the residue for the neat EP and the cured *d*-FREP.

Sample	Wavenumber (cm^{-1})	Assignment
Neat EP	3392	-OH of phenol
	2925	$-CH_3$ and $-CH_2-$
	1607, 1512, 1461	C-C of aromatic ring
	1298	$-CH_2-$
	1180	C-O
Cured d-FREP	908	-P-O-Ph
	973	phosphate
	1437	P-C
	1298	$-CH_2-$ or P=O
	1180	C-O and P-O-Ph
	1450	P-Ph

3.4. Analysis of flame-retardant mechanism in condense phase

The FTIR analysis was carried out to verify the variation of the chemical structure of the epoxy resins at the different temperatures (between 250°C and 550°C) [45]. The data of absorption peaks were presented in Table 5.

At 350°C, the type of the pyrolysis products of the cured *d*-FREP were similar to the pyrolysis products of the cured epoxy resins, as shown in Fig. 7A and B, but the intensities of most peaks of the cured *d*-FREP were decreased and P=O bond was disappeared, which meant that the O=P-O bond in the cured *d*-FREP was less stable than that of the C-C bond [46]. At 450°C, the absorption peaks of $-CH_2$, $-CH_3$ and the aromatic ring of the neat epoxy resins were disappeared, indicating that the main decomposition of the epoxy resins was occurred at this stage. In addition, the peaks of P-C bond and -P-O-Ph bond of the cured *d*-FREP were disappeared at the 450°C, which indicated that the decomposition of the bi-DOPO structure was occurred, as shown in Fig. 7B. At 550°C, compared with the neat epoxy resins, the new peak at 973 cm^{-1} was appeared in the cure *d*-FREP, which indicated that phosphate was formed in the char residue of the cured *d*-FREP. This was mainly because the phosphate produced by the decomposition of the bi-DOPO group can promote the dehydrate and carbonize of the epoxy resins.

In general, the morphology and structure of the carbon layer after combustion can reflect the flammability characteristics of the epoxy resins. The morphology of the char residue after the UL-94 tests was probed by SEM. Some holes and microcracks were showed on the outer and inner surfaces of the char layer of the neat epoxy resins, as shown in Fig. 8A and B. Therefore, flammable volatiles and heat can migrate to the combustion zone through the porous carbon layer. For the cured *d*-FREP, the carbon layers of outer and inner were uniform and dense, which possessed the better barrier effect in condensed phase than that of the neat epoxy resins, as shown in Fig. 8B and D.

The Raman spectroscopy was used to study the graphitization degree of the residual carbon of the cured *d*-FREP. In Fig. 9, there were two characteristic peaks at 1370 cm^{-1} and 1600 cm^{-1} in the

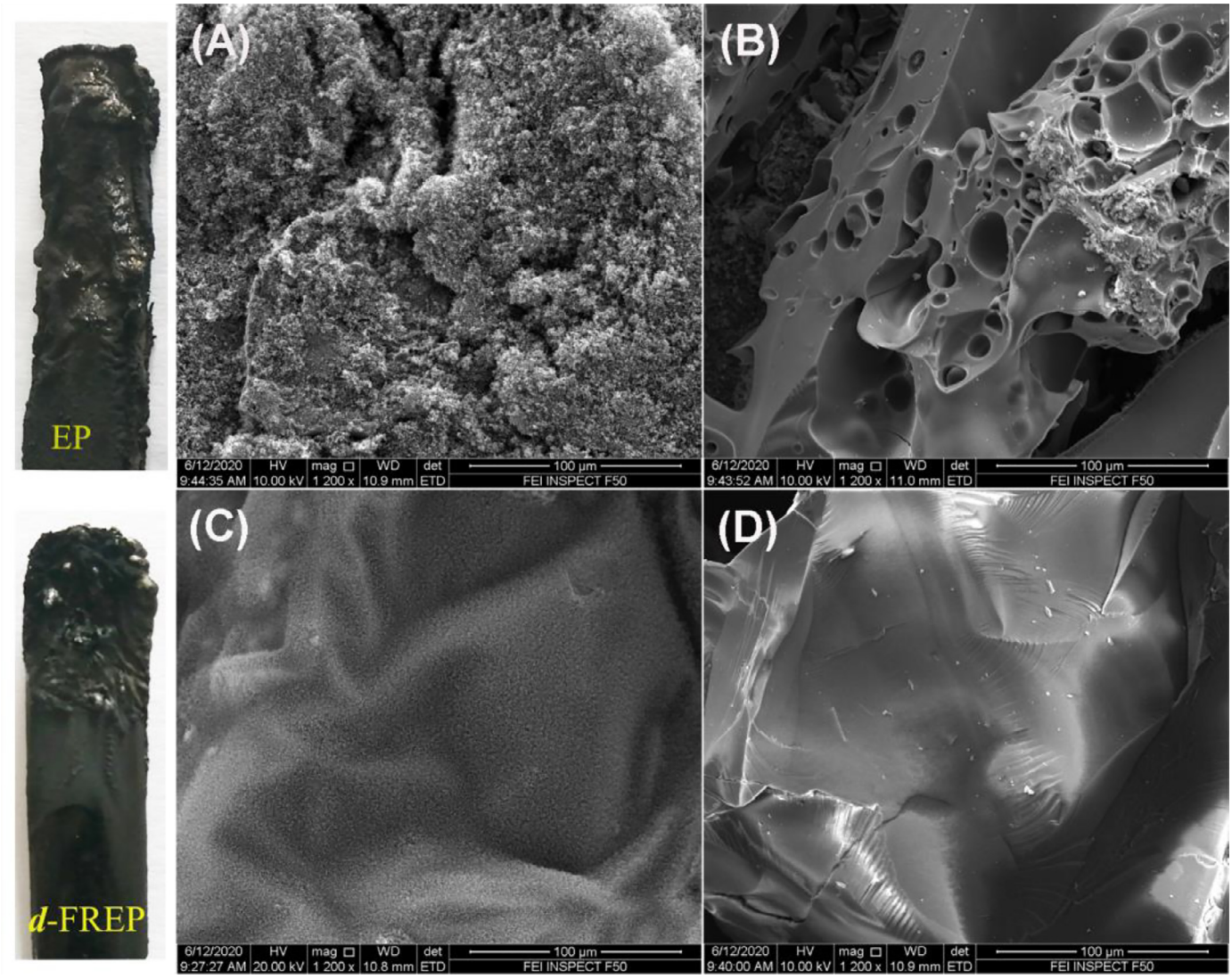

Fig. 8. Scanning electron micrographs and digital image of the residue char after UL-94 test: the outer and inner surface of the neat epoxy resins (A, B) and the cured *d*-FREP (C, D).

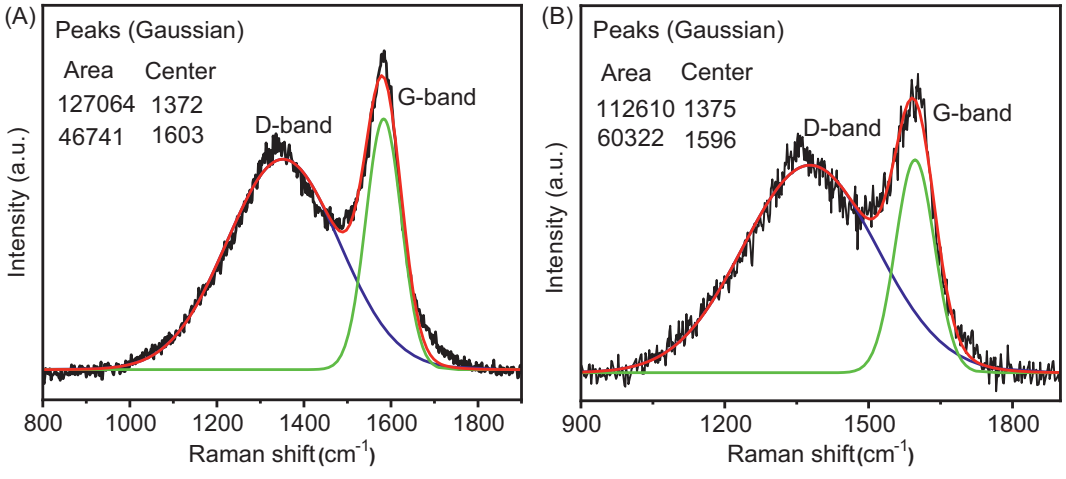

Fig. 9. Raman spectra of char residues: the neat epoxy resins (A) and the cured *d*-FREP (B).

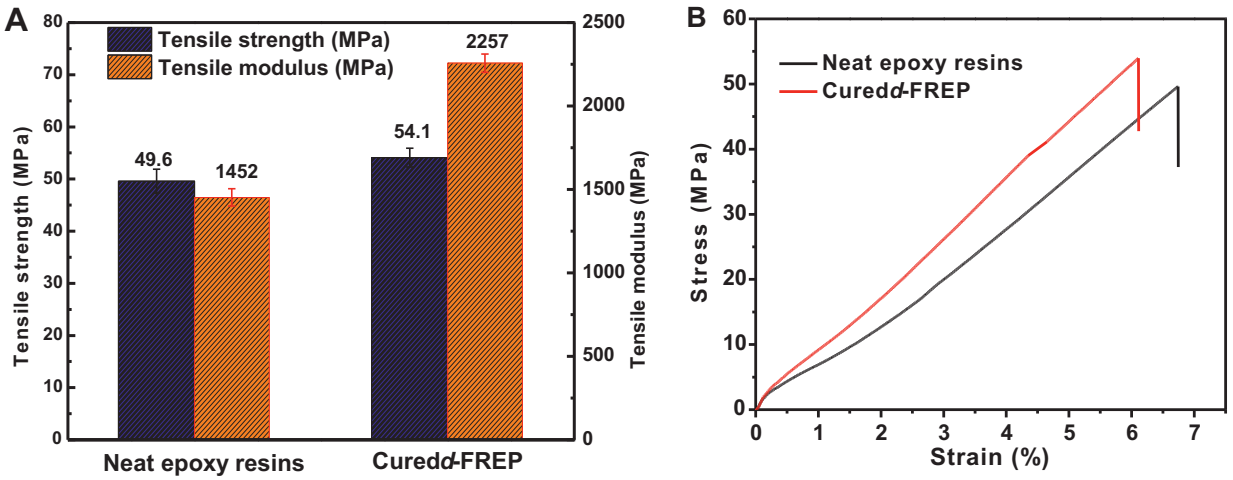

Fig. 10. Tensile strength, tensile modulus (A) and stress-strain curves (B) of the neat epoxy resins and the cured *d*-FREP.

spectrum, which belonged to D and G bands, respectively. Generally, the D band represented the vibration of carbon atoms of the disordered graphite structure. The G band corresponded to the vibration of sp^2-hybridized carbons of the graphite layer. The degree of graphitization was measured using the integrated intensity ratio (I_D/I_G) of the D and G bands [29,34]. Low I_D/I_G ratio meant that the degree of graphitization of carbon was high. The char residue with graphitized structure was regarded as a denser carbonaceous char and an effective barrier [47–50]. The I_D/I_G value of the cured *d*-FREP (1.9) was lower than that of the neat epoxy resins (2.7), which indicated that more char residue with the graphitized structure was formed during the combustion for the cured *d*-FREP, as shown in Fig. 9. This kind of the char residue can slow down the release of burning gas in the combustion process of the cured *d*-FREP.

3.5. Glass transition temperature and mechanical properties of the cured d-*FREP*

The glass transition temperature (T_g) of the cured *d*-FREP and the neat epoxy resins was measured by DSC, and the results were summarized in Table 1. Compared with the neat epoxy resins, the T_g of the cured *d*-FREP increased from 151.9°C to 192.9°C. In general, the T_g of the epoxy resins was depends on its structure of the molecular chain and the substituent [33]. The introduction of rigid biphenyl structure into the epoxy backbone increased the difficulty of chain rotation, hence the T_g of the cured *d*-FREP was higher than that of the neat epoxy resins. In addition, the large-volume DOPO group with strong-polarity was symmetrically distributed on both sides of the molecular chain of the *d*-FREP, which increased the steric hindrance of the chain rotation, thereby the flexibility of the molecular chain was reduced. The T_g of the cured *d*-FREP was higher than that of other epoxy resins systems, as shown in Table 1 [12,40,41].

Fig. 10 presented the tensile properties of the neat epoxy resins and the cured *d*-FREP. As can be seen that the tensile modulus of the cured *d*-FREP (2257 MPa) was higher than that of the neat epoxy resins (1452 MPa), which was attributed to the stronger rigidity of the *d*-FREP molecular segment structure. The cured *d*-FREP possessed higher tensile strength than that of the neat epoxy resins and also the existing flame-retardant epoxy resins [32,51]. This was mainly because the DOPO group was symmetrically distributed around the *d*-FREP molecular chain, resulting in the low mobility of the chain segments. The elongation at break of the cured *d*-FREP (5.7%) was slightly lower than that of the neat epoxy resins (6.8%), as shown in Fig. 10B. The variation of toughness of the cured *d*-FREP was consistent with that of the elongation at break, as shown in Fig. S4.

4. Conclusions

A bi-DOPO type of flame retardancy epoxy prepolymer (*d*-FREP) was synthesized, and its chemical structure was confirmed by ^{1}H NMR, ^{31}P NMR and FTIR. The cured *d*-FREP (phosphorus content: 0.22%) exhibited superior flame retardancy and fire safety compared to the neat epoxy resins. The LOI value of the cured *d*-FREP was increased from 21.0% to 40.0%, and UL-94 test rating was improved from no rating to V-0 rating. Besides, the total heat release of the cured *d*-FREP in the cone calorimeter test was decreased by 64%. The char residue yield of the cured *d*-FREP (28.6%) was higher than that of the neat epoxy resins (11.6%). Compared with the neat epoxy resins, the average effective heat of combustion (av-EHC) of the cured *d*-FREP was decreased by 42%. The flame-retardant mechanism of the cured *d*-FREP was attributed to the flame inhibition of phosphate-containing free radicals in the gas phase and the barrier effect of the dense carbon layer in the condensed phase. The flame inhibition was here the main mechanism of 42% reduction. This indicated that the PO• produced by the pyrolysis of the cured *d*-FREP captured HO• and H• radicals, which inhibited the chain reaction of free radical. Based on the SEM, Raman, and FTIR analysis of the char layers, the bi-DOPO groups promoted the formation of a graphitization char in the *d*-FREP. The cured *d*-FREP possessed a high T_g of 192.9°C, and tensile properties of the cured *d*-FREP was comparable with the neat epoxy resins.

Declaration of Competing Interest

The authors declare that they have no known competing financial interests or personal relationships that can have appeared to influence the work reported in this paper.

Supplementary materials

Supplementary material associated with this article can be found, in the online version, at doi:10.1016/j.polymdegradstab.2021.109629.

CRediT authorship contribution statement

Dongyue Liu: Formal analysis, Data curtion, Writing – original draft. **Pengfei Ji:** Formal analysis. **Tianlong Zhang:** Formal analysis. **Jipeng Lv:** Formal analysis. **Yihua Cui:** Writing - review & editing.

References

[1] H. Jin, G.M. Miller, S.J. Pety, A.S. Griffin, D.S. Stradley, D. Roach, N.R. Sottos, S.R. White, Fracture behavior of a self-healing, toughened epoxy adhesive, Int. J. Adhes. Adhes. 44 (2013) 157–165.

[2] V.H. Pham, Y.W. Ha, S.H. Kim, H.T. Jeong, M.Y. Jung, B.S. Ko, Y.J. Hwang, J.S. Chung, Synthesis of epoxy encapsulated organoclay nanocomposite latex via phase inversion emulsification and its gas barrier property, J. Ind. Eng. Chem. 20 (1) (2014) 108–112.

[3] T.H. Ho, C. Wang, Modification of epoxy resins with polysiloxane thermoplastic polyurethane for electronic encapsulation: 1, Polymer 37 (13) (1996) 2733–2742.

[4] Z. Zheng, Y. Li, S. He, X. Ma, X. Zhu, S. Li, High density and high strength cement-based mortar by modification with epoxy resin emulsion, Constr. Build. Mater. 197 (2019) 319–330.

[5] M.M. Rahman, M.A. Islam, Application of epoxy resins in building materials: progress and prospects, Polym. Bull. (2021) 1–27.

[6] A.B. Morgan, The future of flame retardant polymers-unmet needs and likely new approaches, Polym. Rev. 59 (1) (2018) 25–54.

[7] X. Mu, D. Wang, Y. Pan, W. Cai, L. Song, Y. Hu, A facile approach to prepare phosphorus and nitrogen containing macromolecular covalent organic nanosheets for enhancing flame retardancy and mechanical property of epoxy resin, Compos. Part B-Eng. 164 (2019) 390–399.

[8] J. Qin, W. Zhang, R. Yang, Synthesis of novel phosphonium bromide-montmorillonite nanocompound and its performance in flame retardancy and dielectric properties of epoxy resins, Polym. Compos. 42 (1) (2021) 362–374.

[9] A. Bifulco, D. Parida, K.A. Salmeia, S. Lehner, R. Stämpfli, H. Markus, G. Malucelli, F. Branda, S. Gaan, Improving flame retardancy of in-situ silica-epoxy nanocomposites cured with aliphatic hardener: Combined effect of DOPO-based flame-retardant and melamine, Compos. Part C. 2 (2020) 100022.

[10] A. Bifulco, D. Parida, K.A. Salmeia, R. Nazir, S. Lehner, R. Stampfli, H. Markus, G. Malucelli, F. Branda, S. Gaan, Fire and mechanical properties of DGEBA-based epoxy resin cured with a cycloaliphatic hardener: combined action of silica, melamine and DOPO-derivative, Mater. Design. 193 (2020) 108862.

[11] H. Gan, S.M. Seraji, J. Zhang, S.R. Swan, S. Issazadeh, R.J. Varley, Synthesis of a phosphorus–silicone modifier imparting excellent flame retardancy and improved mechanical properties to a rapid cure epoxy, React. Funct. Polym. (2020) 157.

[12] S. Ma, X. Liu, Y. Jiang, L. Fan, J. Feng, J. Zhu, Synthesis and properties of phosphorus-containing bio-based epoxy resin from itaconic acid, Sci. China Chem. 57 (3) (2014) 379–388.

[13] J. Sag, D. Goedderz, P. Kukla, L. Greiner, F. Schonberger, M. Doering, Phosphorus-containing flame retardants from biobased chemicals and their application in polyesters and epoxy resins, Molecules 24 (2019) 3746.

[14] B. Schartel, A.I. Balabanovich, U. Braun, U. Knoll, J. Artner, M. Ciesielski, M. Doering, R. Perez, J.K.W. Sandler, V. Altstadt, T. Hoffmann, D. Pospiech, Pyrolysis of epoxy resins and fire behavior of epoxy resin composites flame-retarded with 9,10-dihydro-9-oxa-10-phosphaphenanthrene-10-oxide additives, J. Appl. Polym. Sci. 104 (4) (2007) 2260–2269.

[15] C. Schmidt, M. Ciesielski, L. Greiner, M. Doering, Novel organophosphorus flame retardants and their synergistic application in novolac epoxy resin, Polym. Degrad. Stabil. 158 (2018) 190–201.

[16] M. Weinert, O. Fuhr, M. Doering, Novel N-phosphorylated iminophosphoranes based on 9, 10-dihydro-9-oxa-10-phosphapenanthrene-10-oxide, Arkivoc (2018) 278–293.

[17] S. Liang, P. Hemberger, M. Steglich, P. Simonetti, J. Levalois-Grützmacher, H. Grützmacher, S. Gaan, The underlying chemistry to the formation of PO_2 radicals from organophosphorus compounds: a missing puzzle piece in flame chemistry, Chem. Eur. J. 26 (47) (2020) 10795–10800.

[18] S. Wendels, T. Chavez, M. Bonnet, K.A. Salmeia, S. Gaan, Recent developments in organophosphorus flame retardants containing P-C bond and their applications, materials 10 (7) (2017).

[19] S. Ma, Y. Xiao, F. Zhou, B. Schartel, Y.Y. Chan, O.P. Korobeinichev, S.A. Trubachev, W. Hu, C. Ma, Y. Hu, Effects of novel phosphorus-nitrogen-containing DOPO derivative salts on mechanical properties, thermal stability and flame retardancy of flexible polyurethane foam, Polym. Degrad. Stabil. (2020) 177.

[20] K.A. Salmeia, S. Gaan, An overview of some recent advances in DOPO-derivatives: chemistry and flame retardant applications, Polym. Degrad. Stabil. 113 (2015) 119–134.

[21] X. Wang, Y. Hu, L. Song, W. Xing, H. Lu, P. Lv, G. Jie, Flame retardancy and thermal degradation mechanism of epoxy resin composites based on a DOPO substituted organophosphorus oligomer, Polymer 51 (11) (2010) 2435–2445.

[22] B. Schartel, Phosphorus-based flame retardancy mechanisms-old hat or a starting point for future development? Materials 3 (10) (2010) 4710–4745.

[23] A. Battig, P. Müller, A. Bertin, B. Schartel, Hyperbranched rigid aromatic phosphorus-containing flame retardants for epoxy resins, Macromol. Mater. Eng. (2021).

[24] A. Schäfer, S. Seibold, W. Lohstroh, O. Walter, M. Döring, Synthesis and properties of flame-retardant epoxy resins based on DOPO and one of its analog DPPO, J. Appl. Polym. Sci. 105 (2) (2007) 685–696.

[25] J. Artner, M. Ciesielski, O. Walter, M. Döring, R.M. Perez, J.K.W. Sandler, V. Altstädt, B. Schartel, A Novel DOPO-Based Diamine as Hardener and Flame Retardant for Epoxy Resin Systems, Macromol. Mater. Eng. 293 (6) (2008) 503–514.

[26] Y. Liu, Phosphorous-containing epoxy resins from a novel synthesis route, J. Appl. Polym. Sci. 83 (8) (2002) 1697–1701.

[27] Y. Liu, Epoxy resins from novel monomers with a bis-(9,10-dihydro-9-oxa-10-oxide-10-phosphaphenanthrene-10-yl-) substituent, J. Polym. Sci. Pol. Chem 40 (3) (2002) 359–368.

[28] B. Schartel, U. Braun, A.I. Balabanovich, J. Artner, M. Ciesielski, M. Doring, R.M. Perez, J.K.W. Sandler, V. Altstadt, Pyrolysis and fire behaviour of epoxy systems containing a novel 9,10-dihydro-9-oxa-10-phosphaphenanthrene-10-oxide-(DOPO)-based diamino hardener, Eur. Polym. J 44 (3) (2008) 704–715.

[29] Z. Chi, Z. Guo, Z. Xu, M. Zhang, M. Li, L. Shang, Y. Ao, A DOPO-based phosphorus-nitrogen flame retardant bio-based epoxy resin from diphenolic acid: Synthesis, flame-retardant behavior and mechanism, Polym. Degrad. Stabil. 176 (2020) 109151.

[30] S. Jin, Z. Liu, L. Qian, Y. Qiu, Y. Chen, B. Xu, Epoxy thermoset with enhanced flame retardancy and physical-mechanical properties based on reactive phosphaphenanthrene compound, Polym. Degrad. Stabil. 172 (2020) 109063.

[31] C.M. Vu, V.H. Nguyen, Q.V. Bach, Phosphorous-jointed epoxidized soybean oil and rice husk-based silica as the novel additives for improvement mechanical and flame retardant of epoxy resin, J. Fire Sci. 38 (1) (2020) 3–27.

[32] Y. Yan, B. Liang, Flame-retardant behavior and mechanism of a DOPO-based phosphorus–nitrogen flame retardant in epoxy resin, High. Perform. Polym. 31 (8) (2018) 885–892.

[33] A. Battig, J.C. Markwart, F.R. Wurm, B. Schartel, Matrix matters: hyperbranched flame retardants in aliphatic and aromatic epoxy resins, Polym. Degrad. Stabil. 170 (2019).

[34] W. Xie, S. Huang, S. Liu, J. Zhao, Phosphorus-based triazine compound endowing epoxy thermosets with excellent flame retardancy and enhanced mechanical stiffness, Polym. Degrad. Stabil. 180 (2020) 109293.

[35] T. Chen, C. Peng, C. Liu, C. Yuan, J. Hong, G. Chen, Y. Xu, L. Dai, Modification of epoxy resin with a phosphorus, nitrogen, and fluorine containing polymer to improve the flame retardant and hydrophobic properties, Macromol. Mater. Eng. 304 (3) (2018).

[36] C. Liu, T. Chen, C. Yuan, C. Song, Y. Chang, G. Chen, Y. Xu, L. Dai, Modification of epoxy resin through the self-assembly of a surfactant-like multi-element flame retardant, J. Mater. Chem. 4 (9) (2016) 3462–3470.

[37] P. Wang, L. Chen, H. Xiao, T. Zhan, Nitrogen/sulfur-containing DOPO based oligomer for highly efficient flame-retardant epoxy resin, Polym. Degrad. Stabil. 171 (2020) 109023.

[38] D. Sun, Y. Yao, Synthesis of three novel phosphorus-containing flame retardants and their application in epoxy resins, Polym. Degrad. Stabil. 96 (10) (2011) 1720–1724.

[39] W. Xu, A. Wirasaputra, S. Liu, Y. Yuan, J. Zhao, Highly effective flame retarded epoxy resin cured by DOPO-based co-curing agent, Polym. Degrad. Stabil. 122 (2015) 44–51.

[40] Y. Liu, Epoxy resins from novel monomers with a bis-(9,10-dihydro-9-oxa-10-oxide-10-phosphaphenanthrene-10-yl) substituent, J. Polym. Sci. Pol. Chem 40 (3) (2002) 359–368.

[41] P. Deng, Y. Liu, Y. Liu, C. Xu, Q. Wang, Preparation of phosphorus-containing phenolic resin and its application in epoxy resin as a curing agent and flame retardant, Polym. Advan. Technol. 29 (4) (2018) 1294–1302.

[42] B. Schartel, T.R. Hull, Development of fire-retarded materials-Interpretation of cone calorimeter data, Fire. Mater. 31 (5) (2007) 327–354.

[43] L. Liu, Y. Xu, M. Xu, Z. Li, Y. Hu, B. Li, Economical and facile synthesis of a highly efficient flame retardant for simultaneous improvement of fire retardancy, smoke suppression and moisture resistance of epoxy resins, Compos. B Eng. 167 (2019) 422–433..

[44] G. Xu, M. Xu, B. Li, Synthesis and characterization of a novel epoxy resin based on cyclotriphosphazene and its thermal degradation and flammability performance, Polym. Degrad. Stabil. 109 (2014) 240–248.

[45] W. Liang, B. Zhao, C. Zhang, R. Jian, D. Liu, Y. Liu, Enhanced flame retardancy of DGEBA epoxy resin with a novel bisphenol-A bridged cyclotriphosphazene, Polym. Degrad. Stabil. 144 (oct) (2017) 292–303.

[46] X. Wang, Y. Hu, L. Song, W. Xing, H. Lu, Thermal degradation mechanism of flame retarded epoxy resins with a DOPO-substitued organophosphorus oligomer by TG-FTIR and DP-MS, J. Anal. Appl. Pyrol. 92 (1) (2011) 164–170.

[47] Y. Bai, X. Wang, D. Wu, Novel cyclolinear cyclotriphosphazene-linked epoxy resin for halogen-free fire resistance: synthesis, characterization, and flammability characteristics, Ind. Eng. Chem. Res. 51 (46) (2012) 15064–15074.

[48] S. Tang, V. Wachtendorf, P. Klack, L. Qian, Y. Dong, B. Schartel, Enhanced flame-retardant effect of a montmorillonite/phosphaphenanthrene compound in an epoxy thermoset, RSC. Adv. 7 (2) (2017) 720–728.

[49] B. Perret, B. Schartel, K. Stoss, M. Ciesielski, J. Diederichs, M. Doering, J. Kramer, V. Altstadt, Novel DOPO-based flame retardants in high-performance carbon fibre epoxy composites for aviation, Eur. Polym. J. 47 (5) (2011) 1081–1089.

[50] W. Zhang, X. Li, R. Yang, Pyrolysis and fire behaviour of epoxy resin composites based on a phosphorus-containing polyhedral oligomeric silsesquioxane (DOPO-POSS), Polym. Degrad. Stabil. 96 (10) (2011) 1821–1832.

[51] H. Ren, J. Sun, B. Wu, Q. Zhou, Synthesis and properties of a phosphorus-containing flame retardant epoxy resin based on bis-phenoxy (3-hydroxy) phenyl phosphine oxide, Polym. Degrad. Stabil. 92 (6) (2007) 956–961.